

Start-up Scenario in a Helias Reactor

N. Karulin*

IPP 2/337

April 1997



MAX-PLANCK-INSTITUT FÜR PLASMAPHYSIK

85748 GARCHING BEI MÜNCHEN

MAX-PLANCK-INSTITUT FÜR PLASMAPHYSIK

GARCHING BEI MÜNCHEN

Start-up Scenario in a Helias Reactor

N. Karulin*

IPP 2/337

April 1997

**Max-Planck-Institut für Plasmaphysik, EURATOM-Association,
Garching bei München**

*** Nuclear Fusion Institute, Moscow**

*Die nachstehende Arbeit wurde im Rahmen des Vertrages zwischen dem
Max-Planck-Institut für Plasmaphysik und der Europäischen Atomgemeinschaft über die
Zusammenarbeit auf dem Gebiete der Plasmaphysik durchgeführt.*

Abstract

The work presented is devoted to simulation of a stellarator reactor based on the Helias concept with the help of the 1-D time-dependent predictive transport code ASTRA.

The discharges are described by three diffusive equations for the electron density and the electron and ion temperatures. The self-consistent radial electric field is determined from the ambipolarity constraint. A neoclassical transport matrix including non-diagonal elements has been employed. The model of the reactor plasma has been further developed.

A start-up scenario driven by ECR-heating has been calculated. The rise of plasma density is provided by injection of Deuterium-Tritium pellets. The heating power required for ignition and burn coincides with that derived from POPCON calculations.

A regime with a hollow density profile is also presented. The main improvements in the plasma model are described.

Contents

1. Introduction	3
2. Transport Model	4
3. Plasma Model	9
4. Self-Consistent Radial Electric Field	10
5. Model for Pellet Fuelling	13
6. Start-up Scenario for the Helias Reactor	15
7. Regimes with Hollow Density Profiles	22
8. Summary	26

- The new version of the transport equation for particles;
 - The model of the radial electric field has been improved to account for the effect of the radial electric field ($E_r > 0$);
 - The power loss due to fusion reactions has been included;
 - The effect of the radial electric field on the plasma has been included;
 - The model of the radial electric field (laws) and some subroutines has been extended.
- The new version of the development of the earlier work carried out by the Institute for Plasma Physics at the IPP Garching.

1. Introduction

An optimized stellarator of the Helias type is one of the most attractive candidates for a steady state fusion reactor based on the concept of magnetic confinement. Its predecessor, the partly optimized stellarator Wendelstein 7-AS, operating now at the IPP Garching, has demonstrated encouraging experimental results comparable with those of tokamaks. A next-step advanced stellarator, Wendelstein 7-X, is designed to test the reactor potential of the Helias (Helical Advanced Stellarator)¹ concept.

Physical and engineering studies on the Helias reactor have a history of almost ten years. The magnetic configuration, coils and main machine layout have been the dominating issues of these studies. The machine size was chosen on the base of extrapolated scaling laws for the global energy confinement time τ_E in order to obtain ignition and according to the requirement of sufficient space for blanket and shield. The last criterion is rather rigid and one must provide for this purpose a distance of 1.2 - 1.4 m between the coil winding pack and the plasma edge. This value is independent of the reactor type whether stellarator or tokamak. These two main requirements together with numerous detailed optimizations of the magnetic configuration and coils have dictated the choice of a reactor with a major radius of $R = 18 - 22$ m and toroidal magnetic field of $B = 5$ T.

We will consider a reactor with the parameters given below in Table 1, and refer to it as the reference reactor. The goal of the work presented here was to simulate Helias reactor discharges with the help of the 1-D time-dependent transport code ASTRA². Such specific simulations as a start-up scenario with fuelling by pellet injection and gas-puffing and discharges with a hollow density profile have been calculated and are presented in this report.

The plasma model implemented in the ASTRA-code for stellarators has been improved in the following aspects:

- the scenarios were calculated with a transport equation for particles;
- the method to calculate the radial ambipolar electric field has been improved to account for the so-called electron root ($E_r > 0$);
- alpha particle accumulation as a result of fusion reactions has been included;
- fuelling by pellet injection has been included;
- the library of formulas (scaling laws) and some subroutines has been extended.
- This report is a further development of the earlier work carried out by the author during his staying at the IPP Garching.

¹ J.Nührenberg, R.Zille Phys. Lett. A114 (1986) 129

² G.V.Pereverzev, P.N.Yushmanov, A.Yu.Dnestrovskii, A.R.Polevoi, K.N.Tarasjan, L.E.Zakharov Report IPP 5/42, 1991

Table 1 Reference machine and plasma parameters used in the simulations.

Major plasma radius, m	22
Average minor plasma radius, m	1.76
Magnetic field, T	5
Rotational transform $1/2\pi$	≈ 1
Peak plasma temperature, keV	10 - 15
Peak electron density, 10^{20} m^{-3}	< 4
Average beta, %	$\sim 4.5 - 5$
Z_{eff}	2
Fusion power of alpha particles, MW	500 - 700
Fraction of cold alpha particles, %	3 - 5
Plasma heating	< 80 MW ECRH, 140 GHz, on-axis, X-mode

2. Transport Model

In this section the details of the transport model used to simulate the Helias reactor are presented. The optimized magnetic configuration of the Helias reactor contains a relatively small number of dominant Fourier harmonics. When expressed through the magnitude of the magnetic field B , every stellarator configuration can be characterized by the following decomposition:

$$\frac{B}{B_0} = 1 + \sum_{m,l} C_{l,m}(r) \cos m\phi \cos l\theta + \sum_{m,l} S_{l,m}(r) \sin m\phi \sin l\theta, \quad (2.1)$$

where r, ϕ, θ are flux coordinates.

As is seen in Fig.1, the low-number harmonics, especially the harmonics with the toroidal and poloidal numbers $m, l = 0$ and $m, l = 1$ dominate in the magnetic field spectrum of the Helias magnetic configuration. It is an inherent feature of advanced stellarators of the Helias type. This fact allowed the development of an analytic theory of neoclassical transport in the Helias^{3,4,5}. We will write out below a set of formulas according to this neoclassical theory which is employed in the ASTRA-code for the simulation of the reactor.

³ C.D.Beidler, W.D.D'haeseleer Plasma Phys. Control. Fusion **37** (1995) p.463

⁴ C.D.Beidler, W.Lotz, H.Maaßberg In the Proc. of the 21st Europ. Conf. on Contr. Fusion and Pl. Phys., Montpellier, France, 1994, Vol. 18B, Pt II, p.568 (1994)

⁵ C.D.Beidler In the Proceedings of the 6th Workshop on WENDELSTEIN 7-X and Helias reactors. Report IPP 3/331, p.194, 1996

The monoenergetic diffusion coefficient is given as a sum of the stellarator specific term D_h and the term, which is responsible for the transport processes in all axisymmetric toroidal systems (both, stellarators and tokamaks) D_a :

$$D = D_a + D_h. \quad (2.2)$$

The stellarator specific term D_h is expressed as an inverse sum of the terms responsible for the neoclassical transport in different regimes of collisionality:

$$\frac{1}{D} = \frac{1}{D_{1/\nu}} + \frac{1}{D_{\sqrt{\nu}}} + \frac{1}{D_\nu}, \quad (2.3)$$

where $D_{1/\nu}$ is the monoenergetic diffusion coefficient, determining the neoclassical transport in the so-called $1/\nu$ -regime (relatively high collisionality):

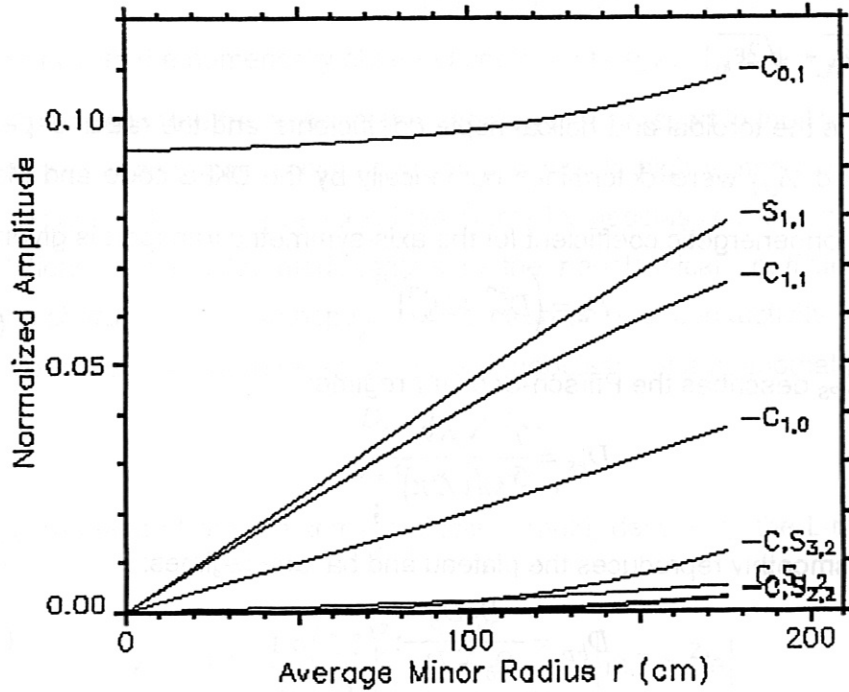


Fig. 1 Fourier coefficients of the magnetic field B as a function of normalized plasma radius for the Helias reactor (kindly provided by J.KiBlinger).

$$D_{1/\nu} = \frac{4}{9\pi} (2\varepsilon_{eff})^{3/2} \frac{v_d^2}{\nu}; \quad (2.4)$$

the term D_ν describes transport in a low collisionality plasma:

$$D_v = A_v \left(\frac{v_d C_{1,0}}{\Omega_E \epsilon_t} \right)^2 \frac{v}{F_{bl}}; \quad (2.5)$$

and the term $D_{\sqrt{v}}$ describes the intermediate region on the collisionality scale:

$$D_{\sqrt{v}} = A_{\sqrt{v}} \left(v_d \frac{C_{1,0}}{\epsilon_t} \right)^2 \frac{\sqrt{v}}{\Omega_E^{3/2}}. \quad (2.6)$$

The notations in the formulas above are:

$$v_d = \frac{(mv^2/2T)T}{qRB} \text{ is the particle drift velocity; } \Omega = qB/m \text{ is the cyclotron frequency;}$$

$\Omega_E = E_r/rB$ is the $E \times B$ precession frequency and E_r is the radial electric field;

$$F_{bl} = \sqrt{\epsilon_t + 2\epsilon_h} - \sqrt{2\epsilon_h},$$

where ϵ_t and ϵ_h are the toroidal and helical ripple coefficients and the radial dependent coefficients ϵ_{eff} , A_v and $A_{\sqrt{v}}$ were determined numerically by the DKES code and Monte Carlo simulations. The monoenergetic coefficient for the axis-symmetric transport is given by:

$$D_a = \left(D_{PS}^{3/2} + D_{bp}^{3/2} \right)^{2/3}, \quad (2.7)$$

where the term D_{PS} describes the Pfirsch-Schlüter regime:

$$D_{PS} = \frac{7}{5} \frac{v_d R v}{\Omega (1/2\pi)^2}; \quad (2.8)$$

and the term D_{bp} smoothly reproduces the plateau and banana regimes:

$$D_{bp} = \frac{D_b D_p}{D_b + D_p}; \quad (2.9)$$

where the banana collisionality regime is described by the coefficient D_b :

$$D_b = \frac{1}{\epsilon_t^{3/2}} \frac{v_d R v}{\Omega (1/2\pi)^2}; \quad (2.10)$$

and for the plateau regime the monoenergetic diffusion coefficient D_p is given by

$$D_p = \frac{2}{5} \frac{v_d v}{\Omega (1/2\pi)}. \quad (2.11)$$

With the help of the monoenergetic transport coefficients the elements of the transport matrix can be derived as follows:

$$D_{n,j} = \frac{2}{\sqrt{\pi}} \int_0^\infty dx_j x_j^{(2n-1)/2} D(x_j) \exp(-x_j), \quad (2.12)$$

where $x_j = \frac{m_j v^2}{2T_j} = \frac{v^2}{v_j^2}$ is the normalized energy and the subscript denotes the particle sort (electrons or ions).

From the expression above the neoclassical diffusion coefficient $D_{nc} = D_1$, the neoclassical thermal conductivity $\chi_{nc} = D_2 - 3D_2/2$ and other elements of the transport matrix can be identified⁶. The equations for the particle and heat fluxes are given now by the formulas:

$$\begin{aligned}\Gamma_j &= -D_1 n_j \left\{ \frac{\dot{n}_j}{n_j} - \frac{q_j E_r}{T_j} + \left(\frac{D_2}{D_1} - \frac{3}{2} \right) \frac{T_j'}{T_j} \right\} \\ Q_j &= -D_2 n_j T_j \left\{ \frac{\dot{n}_j}{n_j} - \frac{q_j E_r}{T_j} + \left(\frac{D_3}{D_2} - \frac{3}{2} \right) \frac{T_j'}{T_j} \right\}.\end{aligned}\quad (2.13)$$

Together with the numerically obtained coefficients e_{eff} , A_n and $A_{\sqrt{n}}$ the above theory is a reliable basis for the treatment of the neoclassical transport in the Helias reactor.

As is well known, the transport properties which high temperature plasmas demonstrate in experiments cannot be explained solely by neoclassical theory. Because of this, the simulations also employ modifications to the neoclassical coefficients, reflecting the anomalous character of the transport. The electron thermal conductivity χ_e and the electron diffusion coefficient D_e were taken as sums of neoclassical and anomalous parts:

$$\begin{aligned}D_e &= D_{nc} + D_{an} \\ \chi_e &= \chi_{nc} + \chi_{an},\end{aligned}\quad (2.14)$$

where χ_{an} was taken from the semi-empirical formula, describing the L-mode in the ASDEX tokamak⁷:

$$\chi_{an} = 1.5 \cdot \frac{1.6 \left(\frac{2.2}{B} \right)^2}{R} \frac{T_e^{3/2}}{(1.1 - (r/a)^2)^4} ; [m, T, m^2/s] \quad (2.15)$$

The thermal conductivity above is based on a random walk model where a step corresponds to the radial widths of the orbits of helically trapped particles in the stellarator. In integral form this model reproduces the Lackner-Gottardi scaling⁷ for the global energy confinement time, τ_{L-G} .

For the anomalous diffusion coefficient D_{an} the same expression was used with a numerical factor in the range from 1/5 to 1/15. The particular coefficient was chosen to maintain the proper ratio of the particle confinement time τ_p to the energy confinement time τ_{L-G} which is expected to be in the range of 3 - 4.

⁶ W.Lotz, J.Nührenberg Phys. Fluids 31, (1988) 2984

⁷ K.Lackner et al. Plasma Phys. and Contr. Fusion 31 No.10, (1989) 1629

To complete the transport formulary we write out below the expressions for the scalings of the global energy confinement time which were used for comparison with the values of τ_E , calculated in the simulations.

The Lackner-Gottardi scaling for stellarators⁸ is given by:

$$\tau_{L-G} = 0.68 \times 0.0627 \times a^2 R B^{0.8} \bar{n}^{-0.6} P^{-0.6} (1/2\pi)^{0.4}; \quad (2.16)$$

the Wendelstein 7-AS scaling⁸ is given by:

$$\tau_{W7AS} = 0.115 \times a^{2.21} R^{0.74} B^{-0.73} \bar{n}^{-0.5} P^{-0.54} (1/2\pi)^{0.43}; \quad (2.17)$$

the LHD-scaling⁸ is given by:

$$\tau_{LHD} = 0.034 \times a^2 R^{0.75} B^{0.84} \bar{n}^{-0.69} P^{-0.58}; \quad (2.18)$$

the ISS95 (International Stellarator Scaling)⁸ is given by:

$$\tau_{ISS95} = 0.079 \times a^{2.21} R^{0.65} B^{0.83} \bar{n}^{-0.51} P^{-0.59} (1/2\pi)^{0.4}; \quad (2.19)$$

the so-called torsatron scaling⁸ is given by:

$$\tau_{tors} = 0.0398 \times a^{2.06} R^{0.74} B^{0.8} \bar{n}^{-0.53} P^{-0.63} (1/2\pi)^{0.39}. \quad 2.20$$

The units in the expressions above are m, T, $10^{19}m^{-3}$, MW, s. Reference⁸ is not the original of all scaling laws above, but all the scalings are collected there.

3. Plasma Model

The model for the reactor plasma includes three differential equations for the electron density n_e , for the electron and ion temperatures T_e and T_i :

⁸ U.Stroth, M.Murakami, R.A.Dory, H.Yamada, S.Okamura, F.Sano, T.Obiki Nucl. Fusion, Vol.36, No.8 (1996), p.1063

$$\begin{aligned}
\frac{\partial}{\partial t}(V n_e) + \frac{\partial}{\partial \rho} \left(V' \langle (\nabla \rho)^2 \rangle \Gamma_e \right) &= V' S \\
\frac{3}{2} \frac{1}{\rho} (V')^{-5/3} \frac{\partial}{\partial t} \left(\rho (V')^{5/3} n_e T_e \right) + \frac{1}{V'} \frac{\partial}{\partial \rho} \left(V' \langle (\nabla \rho)^2 \rangle \left(q_e + \frac{5}{2} T_e \Gamma_e \right) \right) &= P_e \\
\frac{3}{2} \frac{1}{\rho} (V')^{-5/3} \frac{\partial}{\partial t} \left(\rho (V')^{5/3} n_i T_i \right) + \frac{1}{V'} \frac{\partial}{\partial \rho} \left(V' \langle (\nabla \rho)^2 \rangle \left(q_i + \frac{5}{2} T_i \Gamma_i \right) \right) &= P_i
\end{aligned} \tag{3.1}$$

where ρ is the label of the magnetic surface; V is the volume bounded by the magnetic surface with $\rho = \text{const}$ and $V' \equiv \partial V / \partial \rho$. $q_{e,i}$ and $\Gamma_{e,i}$ are the average fluxes of heat and particles. The right sides of the equations above contain total sources and sinks for the particles and heat.

The particle source $S = S_p + S_n$ consists of the sources caused by the pellet injection and of the source arising from the ionization of neutrals coming from outside the plasma edge across the last closed magnetic surface. A special subroutine calculates the radial distributions of the density and temperature of these neutrals, which occur as a result of ionization, recombination and charge-exchange. As input a given density of the neutrals on the magnetic surface with $\rho = a$ was used.

It was assumed that the plasma consisted of the electrons, deuterium and tritium ions in equal amounts and helium ions:

$$\begin{aligned}
n_e &= n_d + n_t + 2n_a \\
n_d &= n_t
\end{aligned} \tag{3.2}$$

The profile of the helium density n_α was taken to be similar to that of the bulk ions, and the total amount of the helium ions has been determined solving the following equation together with the equations (3.2) above:

$$\frac{dn_\alpha}{dt} = n_d n_t \langle \sigma v \rangle_{dt} - \frac{n_\alpha}{\tau_{p,\alpha}} \tag{3.3}$$

where $\langle \sigma v \rangle_{dt}$ is the fusion reaction rate and $\tau_{p,\alpha}$ is the particle confinement time for the helium ions. The latter time was taken as a rule as $\tau_{p,\alpha} = (2-3) \tau_{LG}$ where τ_{LG} is the Lackner-Gottardi scaling for the global energy confinement time. The right sides of the transport equation for the heat contain the terms:

$$\begin{aligned}
P_e &= P_{e,dt} - P_{ei} - P_{br} + P_{ECR} - P_n - P_l - P_{sync} \\
P_i &= P_{i,dt} + P_{ei} - P_{cx}
\end{aligned} \tag{3.4}$$

where the terms $P_{e/ i, dt}$ refer to the heat source owing to high energy alpha particles⁹. There were no direct alpha particle orbit losses in these simulations.

⁹ D.R.Mikkelsen, C.E.Singer, Nucl. Technology / Fusion Vol.4 (1983) p.237

The term P_{ei} is the heat exchange between the plasma electrons and ions due to Coulomb collisions: $P_{ei} = 3n_e(T_e - T_i)m_e/M\tau_{ei}$.

The term P_{br} is the loss due to bremsstrahlung: $P_{br} = 5.06 \times 10^{-5} Z_{eff}^2 n_e^2 T_e^{1/2}$. The term P_{ECR} is the heat source from the electron-cyclotron heating. The ECR-power of the extraordinary wave with the frequency of 140 GHz (fundamental frequency) is absorbed according to the model of single pass resonance¹⁰. On-axis heating is assumed with a peaked model profile of the power deposition: $P_{ECR} \sim (1 - (r/a)^2)^{50}$. The term P_n is the loss due to ionization of the cold neutrals coming from the outside the plasma: $P_n = \langle \sigma_e v \rangle n_n n_e \times 0.013$ keV. P_{sync} is the synchrotron radiation loss¹¹ (it can be neglected at the plasma temperatures typical for the Helias reactor): $P_{sync} = 6.2 \times 10^{-2} \langle n_e \rangle \langle T_e \rangle B^2 \Phi_s$, where Φ_s is the transparency factor. P_{cx} is the energy loss due to charge-exchange with cold neutrals:

$$P_{cx} = 3/2 \langle \sigma_{cx} v \rangle n_n n_i (T_i - T_n).$$

4. Self-Consistent Radial Electric Field

The radial electric field plays a significant role for plasma confinement in the Helias reactor. The situation is different from that of axisymmetric tokamaks, where the particle fluxes are intrinsically ambipolar. In non-axisymmetric stellarators the radial electric field E_r should sustain ambipolarity of the particle fluxes. The latter condition can be expressed by an equation:

$$\sum_j q_j \Gamma_j = 0 \quad (4.1)$$

where the subscript j denotes the particle sort (electrons or ions) and $\Gamma_j(r)$ is the neoclassical particle flux of a species j across a magnetic surface with the normalized radius r . The above equation is valid for steady-state plasmas. It has an algebraic form with respect to E_r and will be used to calculate the ambipolar radial electric field in the Helias reactor. Time independent treatment of the ambipolarity condition implies that the electric field changes faster, than all the plasma parameters.

The equation of ambipolarity (4.1) can in fact have multiple solutions. In such cases there are, as a rule, three solutions, one of which can be excluded as unstable. There is, actually, a specific problem to choose from the remaining two roots. Fortunately, for the typical plasma parameters of the Helias reactor only a single solution -- the negative ion root

¹⁰ O.C.Eldridge, A.C.England Nucl. Fusion, Vol.29 (1989), p.1583.

¹¹ N.A.Ukan ITER Document ITER-TN-PH-8-6 Final Draft, 30 (1988)

-- is expected. This is explained by the fact that the reactor plasmas run at high densities of $n_e(0) = (3 - 4) \times 10^{20} \text{m}^{-3}$ and moderate temperatures of $T(0) = 10 - 14 \text{ keV}$.

The multiple solutions for the electric field arise, however, in some special regimes with a lower plasma density and an intensive on-axis heating. During the start-up phase, when the density is still not high, i.e. $n_e < 2.5 \times 10^{20} \text{m}^{-3}$, and intensive on-axis ECRH heats the plasma electrons up to temperatures of $T_e \sim 9 - 10 \text{ keV}$, conditions for the appearance of the electron root in the vicinity of the plasma axis arise.

It is stated by many authors that solving a differential equation for the radial electric field with a viscous diffusion term leads to a definitive choice of the root (see, for example,¹²). The viscous diffusion term reflects the fact that the particle orbits change their width depending on the spatial derivative of the field E_r . Other problems, however, arise instead of the choice between multiple solutions. To solve the differential equation it is required, first of all, to set up boundary conditions on the plasma axis and on its edge. Defining the latter boundary condition is not entirely obvious.

We have used the algebraic formulation of the ambipolarity condition. It seems to be adequate for the purposes of transport simulation for the Helias reactor, because in most cases only the single ion root exists. The second reason for such an approach is that a procedure for finding the ambipolar electric field should not substantially slow down the calculation process. Investigation of the rather complicated problem of multiple roots of E_r must be specially treated, which can hardly be done in framework of transport simulations.

The neoclassical particle flux is given by^{13,14}

$$\Gamma_j = -D_r n_j \left\{ \frac{n'_j}{n_j} - \frac{q_j E_r}{T_j} + \left(\frac{D_2}{D_1} - \frac{3}{2} \right) \frac{T_j}{T} \right\}, \quad (4.2)$$

where D_1 and D_2 are given by equation (2.12). The prime means the "radial" derivative.

Particle and energy transport in stellarators are found experimentally to be anomalous. On the other hand, mechanisms of the anomalous transport are eventually governed by other than diffusive processes, and it is common to assume that the anomalous transport based on electrostatic fluctuations is intrinsically ambipolar. That is why we consider only the neoclassical fluxes while computing the ambipolar radial electric field.

We comment below briefly on the algorithm for the numerical calculation of the radial electric field E_r . During the runs the ambipolar electric field has been recalculated often enough to ensure smooth time development both of the field itself and of the transport coefficients depending on it. Typically, it was not necessary to recalculate E_r more often than every 10 - 20 ms. In comparison with the global confinement time τ_E for the reactor plas-

¹² D.E.Hastings, W.A.Houlberg and K.C.Shaing: Nuclear Fusion **25** (1985) 445.

¹³ W.Lotz, J.Nührenberg: Physics of Fluids **31** (1988) 2984.

¹⁴ C.D.Beidler, E.Harmeyer, J.Kißlinger, I.Ott, F.Rau, H.Wobig: Report IPP 2/318, 1993.

mas, which is typically of several seconds, this implies good accuracy and allows one to treat the obtained electric field as being ambipolar at every time step.

Let us assume that at the moment t_0 the neoclassical particle fluxes are ambipolar: $\Gamma_e(n^0, T^0, E_r^0) = \Gamma_i(n^0, T^0, E_r^0)$. At the moment $t = t_0 + \Delta t$, where Δt is the time step before recalculating of the electric field, the fluxes are no longer ambipolar, because the plasma density, temperature and collision frequency ν have changed: $\Gamma_e(n, T, E_r^0) \neq \Gamma_i(n, T, E_r^0)$. The radial electric field must be corrected to obtain ambipolarity again: $E_r = E_r^0 + \Delta E_r$. The electron and ion neoclassical fluxes with the new electric field E_r can be written out as follows:

$$\begin{aligned}\Gamma_e &= \Gamma_e(n_e T_e E_r^0) + \frac{\partial \Gamma_e}{\partial E_r} \Delta E_r + \frac{\partial \Gamma_e}{\partial D_{1,2}^e} \frac{\partial D_{1,2}^e}{\partial E_r} \Delta E_r \\ \Gamma_i &= \Gamma_i(n_i T_i E_r^0) + \frac{\partial \Gamma_i}{\partial E_r} \Delta E_r + \frac{\partial \Gamma_i}{\partial D_{1,2}^i} \frac{\partial D_{1,2}^i}{\partial E_r} \Delta E_r \\ \Gamma_e &= \Gamma_i\end{aligned}\quad (4.3)$$

where ΔE_r is the correction to the electric field E_r^0 from the previous time step. The ion transport coefficients $D_{1,2}$ are strongly dependent on the radial electric field. From the above three equations the value ΔE_r can be easily derived:

$$\Delta E_r = \frac{\Gamma_e(n_e T_e E_r^0) - \Gamma_i(n_i T_i E_r^0)}{\frac{\partial \Gamma_i}{\partial E_r} + \frac{\partial \Gamma_i}{\partial D_{1,2}^i} \frac{\partial D_{1,2}^i}{\partial E_r} - \frac{\partial \Gamma_e}{\partial E_r} - \frac{\partial \Gamma_e}{\partial D_{1,2}^e} \frac{\partial D_{1,2}^e}{\partial E_r}} \quad (4.4)$$

The last term in the denominator can be neglected in most cases, since the electron neoclassical coefficients are almost independent of the radial electric field in the plasma parameter range of interest.

This algorithm was implemented in the ASTRA-code and gave satisfactory results. If the electric field changes its sign over the plasma radius at low collisionality, the neoclassical particle flux Γ_e given by this approach is, however, no longer ambipolar in the narrow radial range in which the electric field E_r is small in magnitude.

5. Model for Pellet Fuelling

Sustaining the particle balance in the plasma and the supply of the D-T fuel mixture require a method of plasma refuelling. The high temperature and density plasmas of the Helias reactor can hardly be fuelled by gas-puffing, because the neutrals will be ionized near the

plasma edge. Penetration into the plasma core against the density gradient is questionable in this case. Fuelling by injection of pellets into the reactor plasma partly solves this problem. Moreover, by choosing the pellet size and the pellet velocity it is possible to deposit the density at the required radial position in the plasma.

The fuelling intensity is determined by the rate of particle exhaust from the plasma. The latter is in turn dependent on the total particle loss due to diffusive transport and by the complex processes taking place in the divertor. These two mechanisms are, however, not decoupled from each other.

To evaluate *a priori* the required fuelling rate for the Helias reactor we make a rough estimate. The particle loss rate is equal to

$$\dot{N}_f = \langle n_e \rangle \cdot V_p / \tau_p,$$

where τ_p is the particle confinement time, which can be estimated as $\tau_p \approx (2 - 5) \cdot \tau_E$. If we take for the average plasma density $\langle n_e \rangle$ and for the global energy confinement time τ_E the values expected for the reactor, we will get an estimate for the fuelling rate:

$$\dot{N}_f \approx (4 - 10) \times 10^{22} \text{ s}^{-1}. \quad (5.1)$$

A bigger pellet penetrates deeper into the plasma but the perturbation caused by it is stronger. In the initial phase of the start-up scenario the plasma is too transparent for big and fast pellets. Instead a compromise combination of the pellet parameters r_p , v_p and the injection frequency f_p should be chosen, providing a good ablation profile and an acceptable repetition frequency.

We have used in our simulations an ablation model according to Kuteev¹⁵. The ablation rate of a deuterium pellet is given by the expression:

$$\frac{dN}{dt} = 3.46 \times 10^{14} n_e^{0.453} T_e^{1.72} r_p^{1.443} M_i^{-0.283} \times 0.73, \quad (5.2)$$

where n_e is the electron density in cm^{-3} , T_e is the electron temperature in eV, r_p is the current pellet radius in cm, M_i is mass of the pellet material in atomic units. The factor 0.73 arises due to the fact that the mass of a deuterium atom is more, than that of hydrogen.

The pellet radius r_p decreases according to the formula:

$$r_p^{5/3}(r) = r_p^{5/3}(a) - \frac{5}{3} \frac{M_i^{-1/3}}{4\pi n_p v_p} \int_r^a n_e^{1/3}(r) T_e^{1.64}(r) \cdot dl, \quad (5.3)$$

where r is the current radius in the plasma column, a is the radius of the plasma edge and n_p is the concentration of the atoms in the pellet material. The penetration depth appears at the lower limit of the integration.

After a set of test runs a pellet with the radius of $r_p = 0.375$ cm and with the velocity of $v_p = 6$ km/s were chosen for fuelling the Helias reactor. One pellet deposits into the plasma

$$N_p = \frac{4}{3} \pi r_p^2 \frac{\rho_f}{M_i m_p} = 1.4 \times 10^{22} \quad (5.4)$$

particles, where $\rho_f = 0.258$ g/cm³ is the mass density of the pellet material, m_p is the mass of a proton. This amount is substantially smaller, than the total number of particles in the burning plasma. Now, we can estimate the injection frequency f_p from the expression for the required fuelling rate (5.1) and from the expression (5.4):

$$f_p = \dot{N}_f / N_p = (4-10) \text{ Hz}. \quad (4.5)$$

This estimate is valid for the plasma parameters corresponding to the burning stage of the reactor. A local increase of the plasma density is given by the expression:

$$\Delta n_i = \frac{dN}{dt} \cdot \frac{1}{4\pi r R v_p} \quad (5.6)$$

where the ablation rate should be substituted from the expression (5.2).

All the expressions above are valid for a circular plasma. In our reactor case, when the plasma has a complex non-circular shape, we will use for modeling at this stage a form factor $F = 0.85/1.76 = 0.48$. It roughly takes into account the smaller thickness of the plasma in the bean-shaped cross-section, where the pellet penetrates into the plasma.

A last estimate to be done is the amount of energy needed to ablate the pellet and ionize and heat up the cold ions and electrons from the pellet. Loss of plasma energy to the pellet ablation and ionization can be neglected in our case. Some electron-volts per particle are

¹⁵ B.V.Kuteev Nat. Inst. for Fus. Science Report NIFS-260, 1993

spent for that purpose. On the other hand, the ionized particles must be thermalized in the plasma, and the power required for this is given by

$$P_p = 2N_p \cdot f_p \cdot \langle T \rangle \approx 30 \text{ MW} \cdot f_p, \quad (5.7)$$

where f_p is the injection frequency and $\langle T \rangle$ is the average plasma temperature.

Since all characteristic times concerning the pellet ablation are substantially shorter, than characteristic transport times, the ablation and ionization are assumed to be instantaneous.

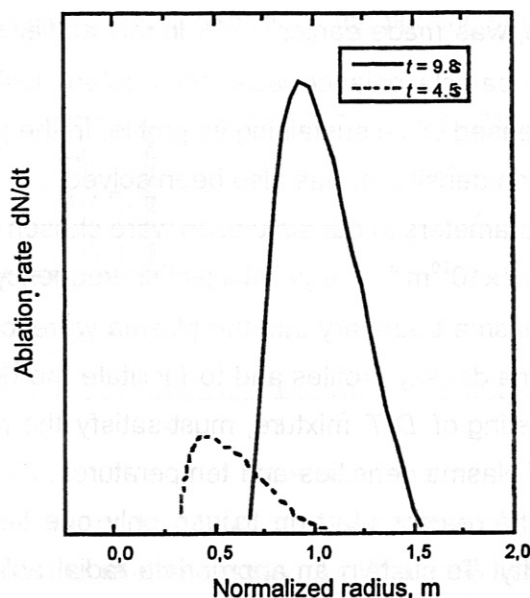


Fig. 2 Ablation rate profiles in the Helias reactor according to expression (5.2) at two moments of the start-up scenario. At $t = 4.5$ s the peak values were: $n_e = 3.65 \times 10^{20} \text{ m}^{-3}$, $T_e = 9.4$ keV; at $t = 9.8$ s the peak values were $n_e = 3.9 \times 10^{20} \text{ m}^{-3}$, $T_e = 12.3$ keV. The ablation profiles calculated for the Helias reactor plasma are shown in Fig.2.

6. Start-up Scenario for the Helias Reactor

The scenario examined in the scope of this work is based on electron cyclotron resonance heating by the extraordinary wave at the fundamental frequency of 140 GHz and based on the fuelling by means of pellet injection. To obtain a steady-state burning plasma, one should be convinced that the operational point is achievable with a given heating power. This means, in fact, that a set of scenarios with different heating powers must be calculated before an optimal variant is developed.

ECR-heating has been widely used in stellarator experiments, and the progress in development of powerful gyrotrons promises that generators with the needed parameters will

be available in the near future. The extraordinary wave proposed for the Helias has an extremely high cut-off plasma density of $4.8 \times 10^{20} \text{ m}^{-3}$, which is especially advantageous for the stellarator reactor. However, the wave should be launched into the plasma from the high field side.

The plasma density must also be raised up to the values needed for burn. The injection of pellets seems to be the only tool to fuel dense, high temperature reactor-grade plasmas.

A first attempt to model start-up scenarios for the Helias reactor, using for that purpose the ASTRA transport code, was made earlier^{16,17,18}. In this earlier study the plasma density profile was fixed and the particle balance was not treated. Instead, the density of the plasma was gradually increased while sustaining its profile. In the present report, the transport equation for the electron density n_e has also been solved.

The starting plasma parameters in our simulation were chosen as follows: $T_e(0) = T_i(0) = 1.3 \text{ keV}$, $n_e(0) = n_i(0) = 1.7 \times 10^{20} \text{ m}^{-3}$. The pellet injection frequency and the intensity of the neutral flow through the plasma boundary into the plasma were controlled manually during the runs to obtain flat plasma density profiles and to facilitate the density rise. The size and velocity of the pellet, consisting of $D-T$ mixture, must satisfy the requirements of good absorption in a wide range of plasma densities and temperatures. Actually, it is not quite adequate for the purpose of the reactor start-up to use only one set of pellet injectors with fixed pellet size and velocity. To sustain an appropriate radial ablation profile, it would be extremely desirable to have at least two injectors (or, groups of injectors) shooting the pellets of different sizes and with different velocities. The slower and smaller pellets should be used for the very beginning of the discharge, when the plasma has lower parameters (n , T), and the other for the later phase of the scenario, including the regime with burning plasma.

The injected pellets should not substantially disturb the plasma, i.e. the number of particles in the pellet should be small compared to the number of the bulk plasma ions or electrons: $N_p = 4/3\pi r_p^3 n_p \ll \langle n_e \rangle V_{pl}$, where r_p and n_p are the radius of the pellet and concentration of the atoms in it, and $\langle n_e \rangle$, V_{pl} are the average plasma density and the plasma volume of the reactor.

A $D-T$ pellet (50 - 50 mixture), which more or less fulfills all the requirements mentioned above, has the radius of $r_p = 0.375 \text{ cm}$ and should be injected into the plasma with the velocity of 6 km/s . The inverse injection frequency varied from $\Delta t = 0.5 \text{ s}$ to 0.1 s .

The ECR-heating was deposited on the axis of the discharge. The absorption of the wave was calculated continuously in time according to the model of single path absorption

¹⁶ N.E.Karulin, Report IPP 3/328, 1994

¹⁷ In the Proceedings of the 6-th Workshop on WENDELSTEIN 7-X and Helias Reactors, F.Rau, F.Hernegger (Editors), Report IPP 2/331, 1996, p.215

of a pencil wave¹⁰. In this approximation the wave is totally absorbed in the plasma. The deposition profile of the wave was approximated by a curve $\Delta P/\Delta V \sim (1 - r/a)^{50}$, where r is the current normalized plasma radius, a is the radius of the last closed magnetic surface and $\Delta P/\Delta V$ is the ECR-power released in the plasma volume ΔV .

The electron cyclotron power needed for achieving ignition and burn was obtained from numerous runs and its value of $P_{ECR} = 74$ MW coincides with that calculated from the simplified zero dimensional estimates¹⁸. At the very beginning, however, the heating power was lower, namely, 54 MW. Total time needed to reach the burning state was about 10 s.

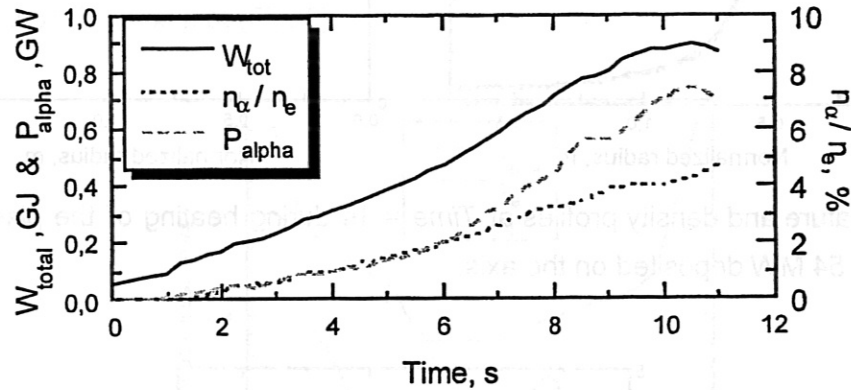


Fig. 3 Time development of the plasma total energy content W_t , fusion power released in alpha particles P_{alpha} and of the relative density of cold alphas in the plasma n_{α}/n_e

During the initial heating up phase the profiles of the electron and ion temperatures were rather peaked (see Fig. 4 below), because the ECR-power is deposited in a narrow resonance zone on the axis of the discharge.

¹⁸ C.D.Beidler, G.Grieger, E.Harmeyer, J.Kißlinger, N.Karulin, W.Maurer, J.Nührenberg, F.Rau, J.Sapper, H.Wobig, Report IPP 2/330, 1995

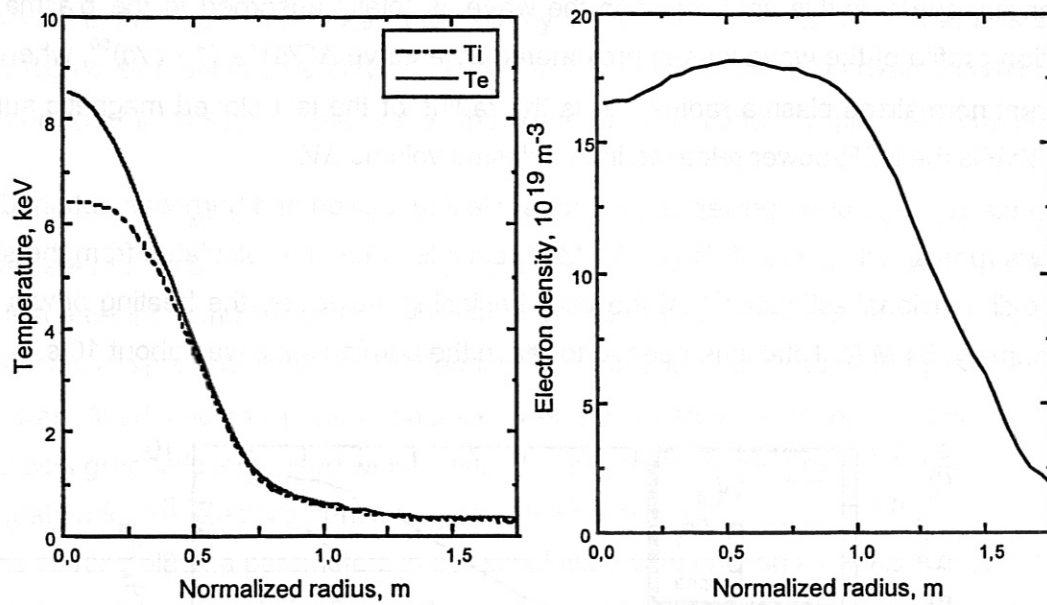


Fig. 4 Temperature and density profiles at *Time* = 1s during heating of the plasma with the ECR-power of 54 MW deposited on the axis.

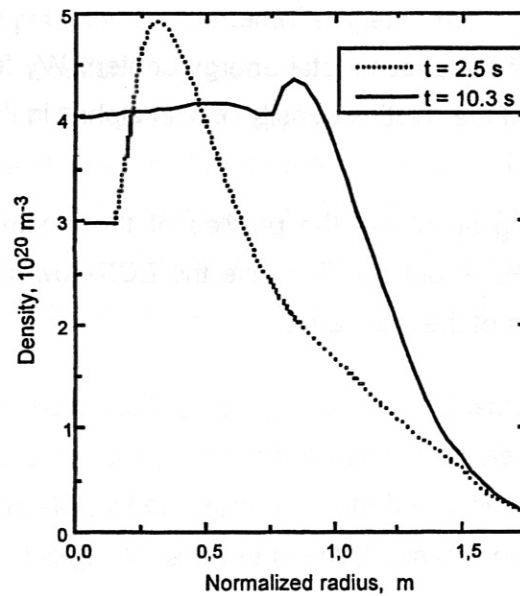


Fig. 5 The profile of the electron density just after pellet ablation at the moments *Time* = 2.5s and 10.3s.

The pellet injected into the plasma just after the moment *Time* = 1 s cools down the plasma and builds up the density in its inner region. The pellet with the parameters chosen above disappears as a result of ablation when it has already passed the axis, because the low density plasma is not optically thick enough. Two typical profiles of the electron density just after the pellet ablation at the initial phase of the heating up and at the operational point are demonstrated in Fig. 5.

The process of building up the temperature develops in the following manner. The on-axis plasma quickly becomes relatively hot, owing to the localized powerful electron-cyclotron heating, but the outer plasma remains at the same time cool. The hot boundary with a high temperature gradient moves slowly towards the plasma edge. Since the electron-cyclotron wave is the dominating heating source at that time, and the fusion power is still low, smoothing the temperature profiles is caused solely by transport processes. The flow of heat outwards is hampered by the low thermal conductivity due to the low plasma temperatures in the non-resonant regions, where ECR-heating does not take place. For example, the profiles of the thermal conductivities corresponding to the previous plots (Fig. 4) are presented on the next plot (Fig. 6).

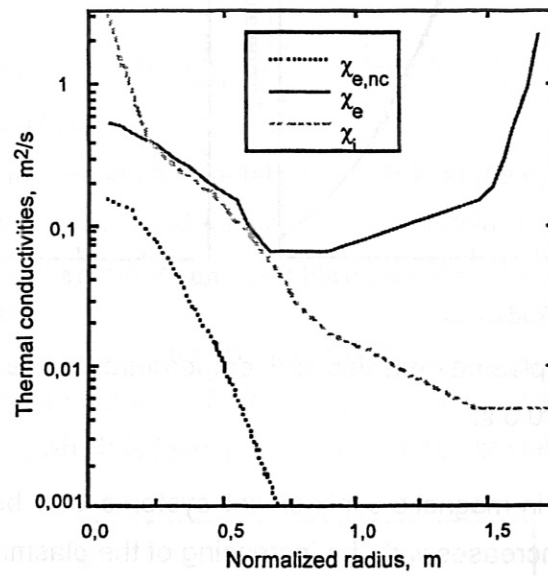


Fig. 6 Thermal conductivities at the moment $Time = 1s$: χ_i is the neoclassical ion thermal conductivity, $\chi_{e,nc}$ is the neoclassical and χ_e is the total (n.c. + anomalous) electron thermal conductivity.

Together with the rise of the ion temperature near the axis, the alpha particle fusion power P_{alpha} , which is approximately proportional in that parameter range to $n_i^2 T_i^3$, gradually heats up the plasma in a wider radial zone. At the moment $Time = 7.8 s$ the power density of the alpha heating reaches that of the ECR-heating even on the plasma axis. At this step the heating power was reduced to 38 MW and after another 2 s was switched off. A step on the curve $P_{alpha}(t)$ after the moment of decreasing the heating at $Time = 7.8 s$ shows that the alpha particle heating almost stops its growth, but then increases again. From that time the discharge is self sustaining. The discharge just into the 10th second can be treated as an operational point.

The profiles of the temperatures and plasma densities are demonstrated in Fig. 7; the main global parameters are presented in Table 2, below. Despite the fact that the pellets penetrate into the plasma only up to the radius of $r = 0.8a$, (s. Fig. 5), it is possible to maintain a flat density profile. The plasma parameters obtained and the fusion power are close to the reference ones.

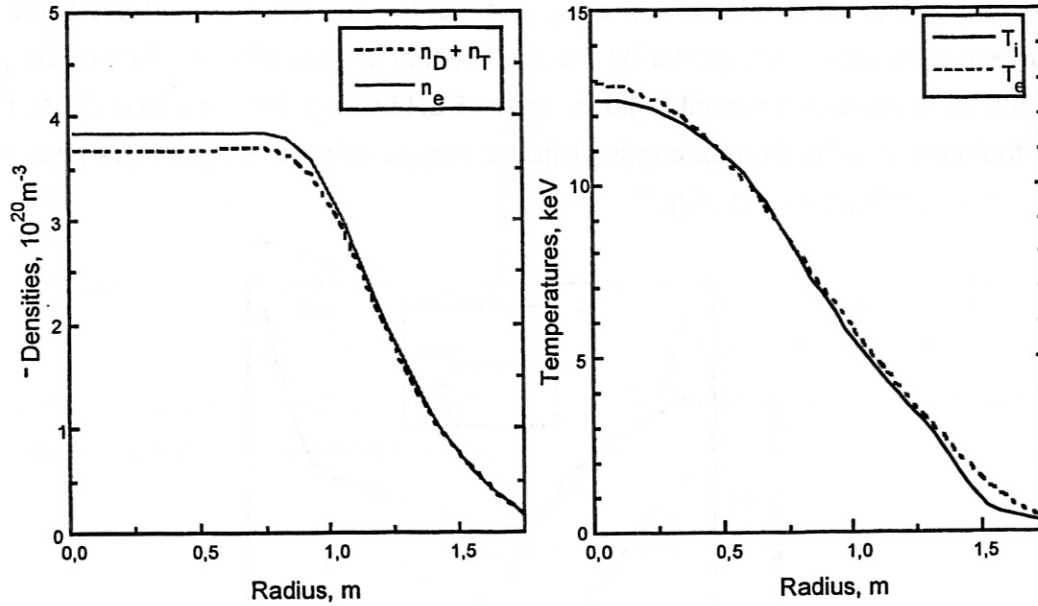


Fig. 7 Profiles of the plasma densities and temperatures of the operational point at the moment $Time = 10.3$ s.

Thermonuclear burn in magnetic confinement systems can be thermally unstable, because the reaction rate increases with the increasing of the plasma temperature. It was not the purpose of this simulation to develop a method or an algorithm to stabilize the operational point. Nevertheless, it was found that thermal run-away of the Helias reactor can be avoided by controlling the injection frequency of the pellets.

The transport properties of the burning plasma can be characterized by the plots of the thermal conductivities and of the ambipolar radial electric field E_r given below (Fig. 8). In spite of the fact that the negative ion root of the electric field takes place here, the transport properties of the optimized Helias configuration are good. We should point out that no enhanced confinement was assumed in this simulation. The anomalous electron thermal conductivity was taken to be of the ASDEX-like L-mode⁷ form

$$\chi_{an} = 1.5 \cdot \frac{1.6 \left(\frac{2.2}{B} \right)^2}{\left(1.1 - (r/a)^2 \right)^4} \frac{T_e^{3/2}}{; [m, T, m^2/s]}$$

The anomalous fraction of the electron thermal conductivity at the axis exceeds the neoclassical one by a factor of 2.3 and the ion thermal conductivity is larger at the axis than that of the electrons.

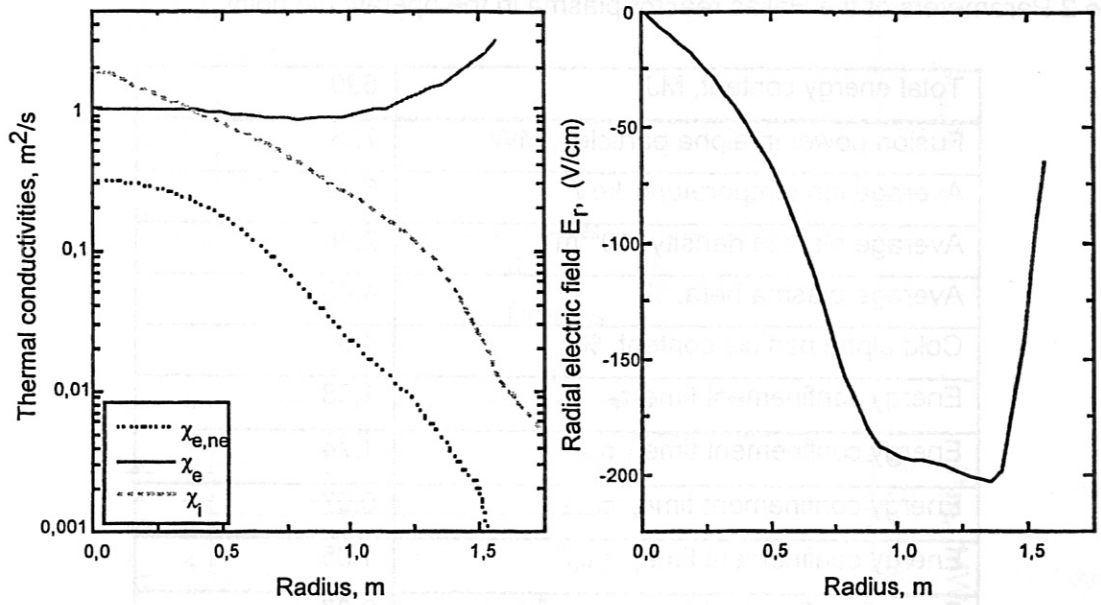


Fig. 8 Thermal conductivities and the radial electric field at the operational point of the Helias reactor. χ_i is the neoclassical ion, $\chi_{e,nc}$ is the neoclassical electron and χ_e is the total (neoclassical + anomalous) electron thermal conductivity.

The last plot, which is of interest for the MHD stability of the plasma, demonstrates the profile of the plasma toroidal beta (Fig. 9). The slope of the beta profile is almost constant over the normalized radius, which is favorable from the point of view of MHD-stability.

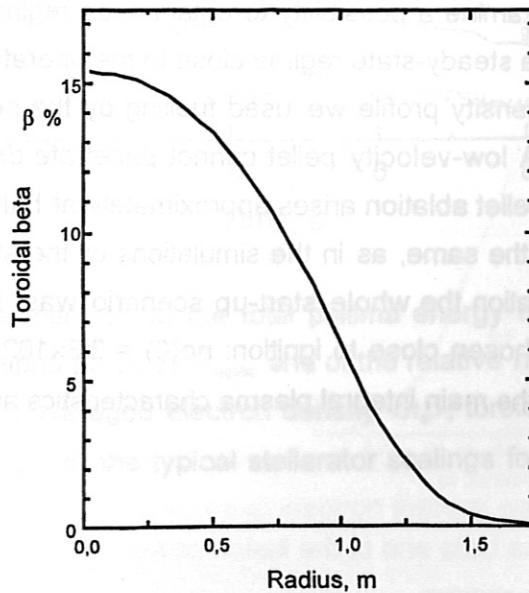


Fig. 9 Beta profile at the operational point of the reactor.

Table 2 Parameters of the Helias reactor plasma in the operational point.

Total energy content, MJ	890
Fusion power in alpha particles, MW	725
Average ion temperature, keV	6.72
Average plasma density, 10^{20}m^{-3}	2.76
Average plasma beta, %	4.60
Cold alpha particle content, %	4.5
Energy confinement time τ_E	1.68
Energy confinement time, τ_{L-G}^8	1.74
Energy confinement time, τ_{ISS95}^8	0.97
Energy confinement time, τ_{LHD}^8	1.05
Energy confinement time, τ_{W7AS}^8	2.07

7. Regimes with Hollow Density Profiles

Discharges with hollow profiles of the plasma density are one of the typical regimes in modern experiments with ECR-heating, for example, on partly optimized stellarator Wendelstein 7-AS. They have some physical advantages, which we are not able to discuss here, and it was of interest to examine a possibility to obtain such regimes in the Helias reactor. The goal was to try to find a steady-state regime close to the operational regime

To produce a hollow density profile we used fuelling by the pellets with a reduced injection velocity of 4 km/s. A low-velocity pellet cannot penetrate deep into the plasma, and the particle source due to pellet ablation arises approximately at half the plasma radius. The size of the pellet remained the same, as in the simulations of the start-up scenario, namely $r_p = 0.375$ cm. In this simulation the whole start-up scenario was not calculated, the initial plasma parameters were chosen close to ignition: $n_e(0) = 3.3 \times 10^{20} \text{m}^{-3}$, $T_e(0) = T_i(0) = 10$ keV. Time development of the main integral plasma characteristics are plotted in Fig. 10.

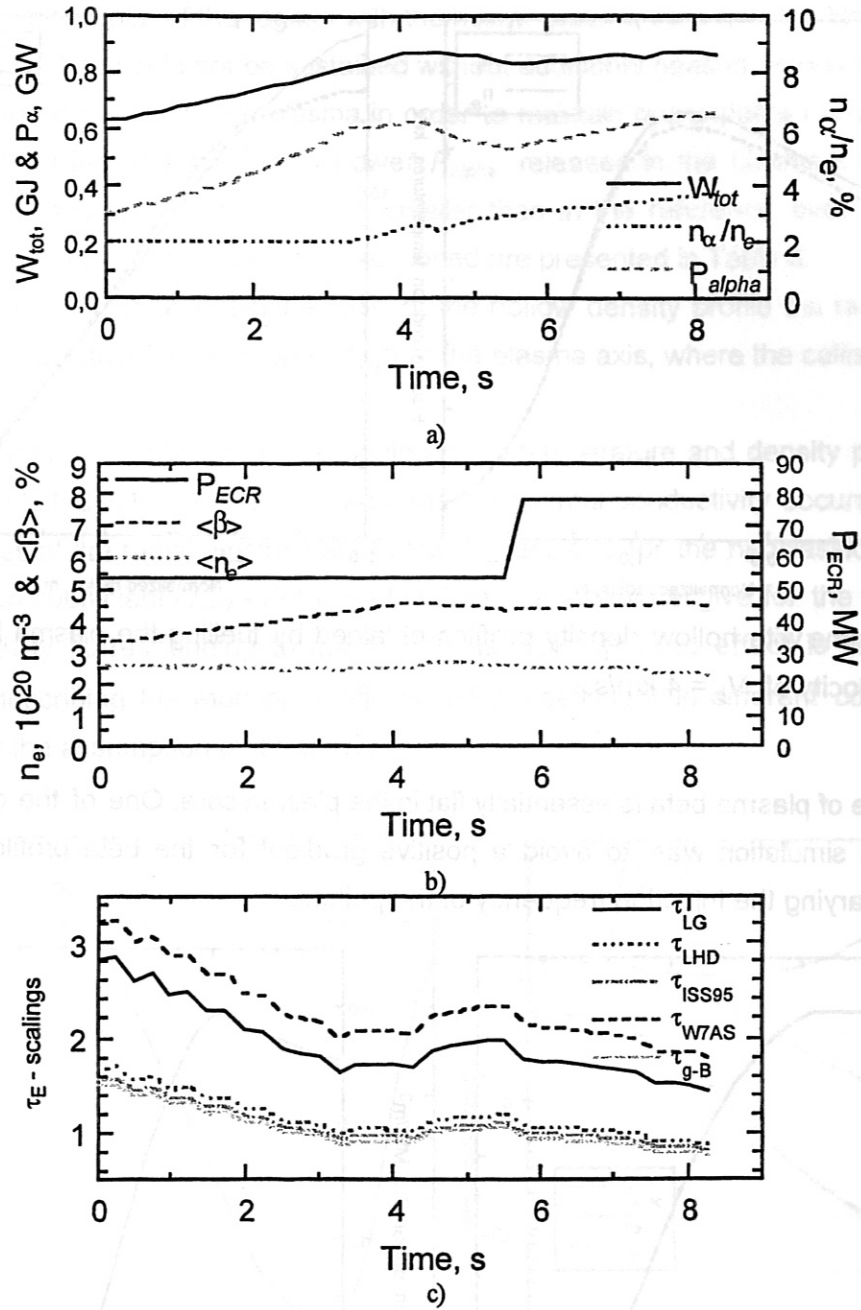


Fig. 10 Time development of a) the total plasma energy content W_{tot} , fusion power released in alpha particles P_{α} and of the relative helium concentration n_{α}/n_e ; b) the volume-averaged electron density $\langle n_e \rangle$, toroidal beta $\langle \beta \rangle$ and of the ECR-heating P_{ECR} ; c) the typical stellarator scalings for the global energy confinement time τ_E .

The following plots present a quasi-equilibrium state of the D-T plasma:

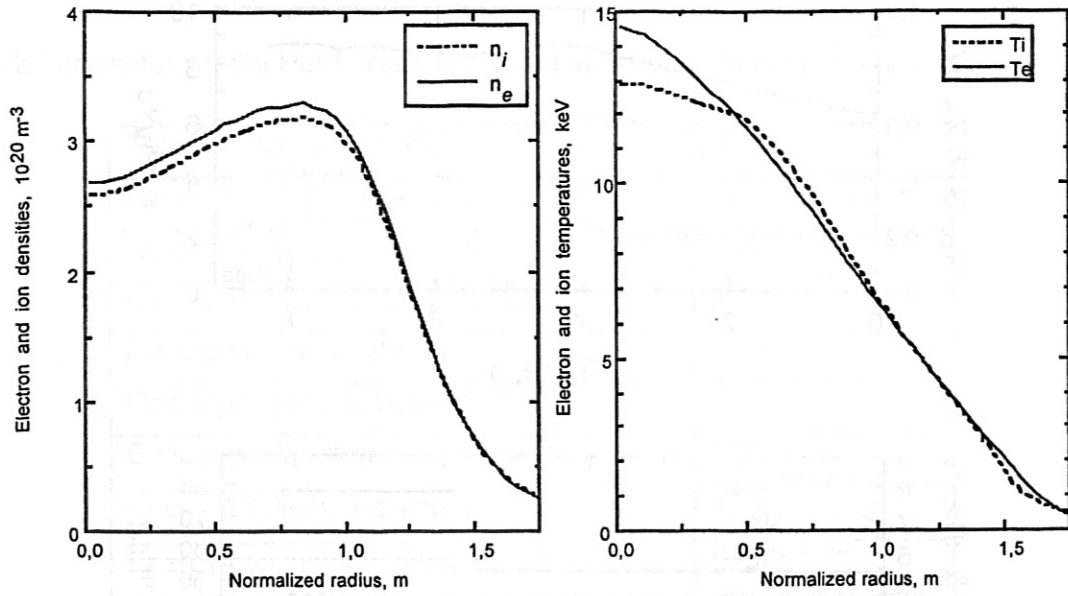


Fig. 11 Regime with hollow density profiles obtained by fuelling the plasma by pellets with the velocity of $V_p = 4 \text{ km/s}$.

The profile of plasma beta is essentially flat in the plasma core. One of the control criteria during this simulation was to avoid a positive gradient for the beta profile. This was achieved by varying the injection frequency of the pellets.

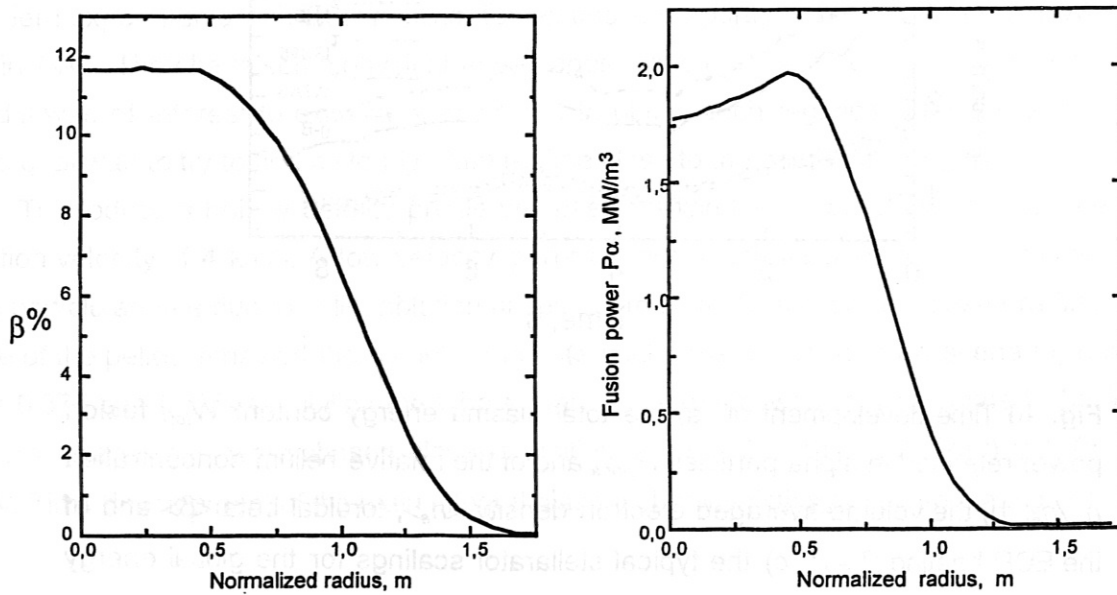


Fig. 12 Profiles of plasma beta and of the fusion power released in alpha particles for the hollow density profile regime.

The main difference of the regime with the hollow plasma density in the Helias reactor is that the steady-state could not be sustained without additional heating. Power of $P_{\text{ECR}} = 50 - 70$ MW had to be applied to the plasma in order to maintain quasi-stable burn. This can be explained by the fact that the fusion power P_{alpha} released in the plasma core when the density profile is hollow is a factor 1.5 smaller than in the reference case. Other global plasma parameters of the two regimes mentioned are presented in Table 3.

It is interesting to note that in the case of the hollow density profile the radial ambipolar electric field is positive (an electron root) near the plasma axis, where the collisionality is the lowest.

The thermal conductivities corresponding to the temperature and density profiles above (Fig. 11) are plotted in Fig. 13. The peak on the ion thermal conductivity occurs, because at the low values of the radial electric field E_r , the expressions for the neoclassical monoenergetic diffusion coefficient (2.3) - (2.6) used in the transport model give for the ions the thermal conductivity corresponding to the $1/\nu$ -regime. This spurious effect is caused by the method of describing the monoenergetic diffusion coefficient in different collisionality regimes under the assumption of „large“ E_r .

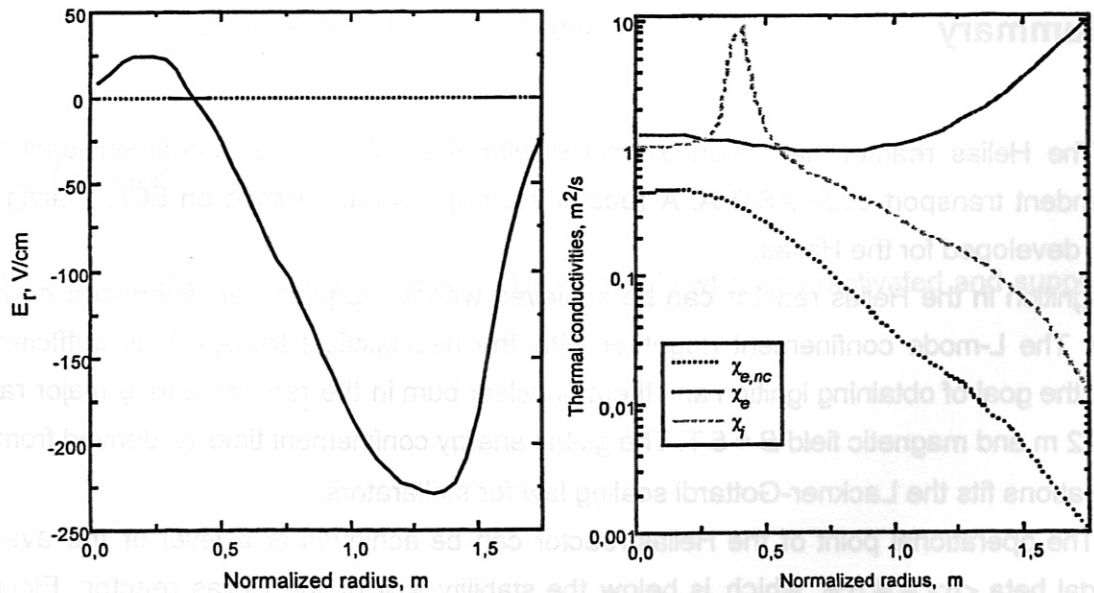


Fig. 13 Radial electric field E_r and the thermal conductivities in the discharge with the hollow density profile. χ_i is the neoclassical ion, $\chi_{e,nc}$ is the neoclassical electron and χ_e is the total (neoclassical + anomalous) electron thermal conductivity.

Table 3 Global plasma parameters for two regimes of the Helias reactor: a) with a standard density profile; b) with a hollow density profile and ECR-heating of $P_{\text{ECR}} = 74$ MW.

	a)Reference case	b)Hollow density
Total energy content, MJ	890	874
Fusion power in alpha particles, MW	725	650
Average ion temperature, keV	6.72	7.35
Average plasma density, 10^{20}m^{-3}	2.76	2.32
Average plasma beta, %	4.60	4.51
Cold alpha particle content, %	4.5	3.6
Energy confinement time τ_E	1.68	1.49
Energy confinement time, τ_{L-G}^8	1.74	1.51
Energy confinement time, τ_{ISS95}^8	0.97	0.85
Energy confinement time, τ_{LHD}^8	1.05	0.90
Energy confinement time, τ_{W7AS}^8	2.07	1.84

8. Summary

The Helias reactor has been examined with the help of the one-dimensional time-dependent transport code ASTRA. A reactor start-up scenario based on ECR-heating has been developed for the Helias.

Ignition in the Helias reactor can be achieved without requiring an enhanced confinement. The L-mode confinement (together with the neoclassical transport) is sufficient to meet the goal of obtaining ignition and thermonuclear burn in the reactor with a major radius $R = 22$ m and magnetic field $B = 5$ T. The global energy confinement time τ_E derived from the simulations fits the Lackner-Gottardi scaling law for stellarators.

The operational point of the Helias reactor can be achieved at a level of the average toroidal beta $\langle\beta\rangle \sim 4.5\%$, which is below the stability limit of the Helias reactor. Electron-cyclotron power of about $P_{ECR} \sim 70 - 80$ MW applied at the plasma axis seems to be sufficient to heat up the reactor plasma to ignition. This value, obtained in numerous time-dependent simulations, demonstrates a good correspondence with the previous results of zero dimensional analysis on the base of empirical scaling laws (POPCON-analysis).

The radial electric field, which was calculated self-consistently, remains in most cases negative (ion root). The electron root appears near the plasma axis in the regimes with lower electron density ($n_e < 2.5 \times 10^{20}\text{m}^{-3}$) and high plasma temperature -- a low collisionality regime.

The particle transport and particle balance based on the neoclassical theory for advanced stellarators were treated for the first time in the modeling of Helias reactor discharges. Anomalous losses were also taken into account. The model included particle sources from the neutrals coming from the edge and from the injected pellets.

Fuelling by means of injection of pellets was applied in the Helias reactor simulations to build up the plasma density. It appears to be an appropriate method to create and sustain both flat and hollow density profiles. It has been also found that this fuelling method can be useful in controlling the burn. Decreasing the injection frequency leads, as a rule, to suppressing the self-sustaining burn, because the plasma density decreases and, hence, the fusion power released by the alpha particles decreases as well.

Time-dependent accumulation of the cold alpha particles (helium) was included into the plasma model. This effect influences the thermal stability of the burning plasma because of the delay in stabilizing the helium content in the plasma caused by a relatively long characteristic particle time, which exceeds the global energy confinement time: $\tau_{p,He} > \tau_E$.

Regimes with hollow density profiles were simulated. Under these conditions it was found that the reactor plasma cannot be maintained in a burn steady-state at values of average beta of $\langle \beta \rangle \sim 4.5\%$ without additional heating. The positive electron root of the radial electric field arises at the plasma axis in these regimes.

Acknowledgments

I would like to express my gratitude to Dr. H. Wobig who has motivated and supported this work.